

Improved Thermoelectric Power Factor in Metal-Based Superlattices

Daryoosh Vashaee and Ali Shakouri*

Jack Baskin School of Engineering, University of California, Santa Cruz, California 95064, USA

(Received 16 May 2003; published 11 March 2004)

In this paper we present a detailed theory of electron and thermoelectric transport perpendicular to heterostructure superlattices. This nonlinear transport regime above barriers is also called heterostructure thermionic emission. We show that metal-based superlattices with tall barriers can achieve a large effective thermoelectric figure of merit ($ZT > 5$ at room temperature). A key parameter to achieving high performance is the nonconservation of lateral momentum during the thermionic emission process. Conservation of lateral momentum is a consequence of translational symmetry in the plane of the superlattice. We also discuss the use of nonplanar barriers and embedded quantum dot structures to achieve high thermoelectric conversion efficiency.

DOI: 10.1103/PhysRevLett.92.106103

PACS numbers: 68.60.Dv, 73.50.Lw

The thermoelectric figure of merit (ZT) is determined by a dimensionless parameter $ZT = \sigma S^2 T / \beta$, where T is the temperature, σ and β are the electrical and thermal conductivities of the material, respectively, and S is the Seebeck coefficient. A good thermoelectric material should have high electrical conductivity to minimize Joule heating, low thermal conductivity to prevent thermal shorting, and a high Seebeck coefficient for maximum conversion of heat to electrical power or electrical power to cooling. The thermoelectric material most often used in today's Peltier coolers is an alloy of bismuth telluride (Bi_2Te_3) with $ZT \sim 1$. In addition to bismuth telluride, there are other thermoelectric materials including lead telluride (PbTe), silicon germanium (SiGe), and bismuth-antimony (Bi-Sb) alloys that are used at various operating temperatures. There have been two recent reports by Venkatasubramanian *et al.* [1] and Harman *et al.* [2] on materials with $ZT \sim 2$ – 2.4 at room temperature, where the main improvement comes from the reduction in lattice thermal conductivity.

Vacuum thermionic coolers were first proposed by Mahan in 1994 [3]. They can achieve high efficiencies ($> 80\%$ of Carnot value) but since stable low work function material is not available, their use is limited to high temperatures (> 500 K). Shakouri *et al.* first proposed to use thermionic emission in heterostructures for cooling applications at room temperature [4,5]. The main emphasis was on nonlinear transport regime and high cooling power density (> 100 W/cm²). However, designs that could achieve high efficiency were not considered. Another advantage of heterostructure integrated thermionic (HIT) coolers is their reduced material requirements. Low thermal conductivity and high electrical conductivity barrier material is needed; however the requirement for a large bulk Seebeck coefficient is reduced since the barrier height is another parameter to control cooling at interfaces. Subsequent studies of HIT coolers showed that despite the nonlinearity of the trans-

port equations, material figure of merit is similar to conventional bulk thermoelectric materials and it is $m^* \mu^{3/2} / \beta$, where m^* is the effective mass, μ is the mobility, and β the thermal conductivity of the barrier material [6,7]. Increasing the efficiency (ZT) value using multilayer thermionic emission was first proposed by Mahan *et al.* [8]. Based on this idea, a few structures were synthesized by Kim *et al.*; however due to poor material quality no improvement was reported [9]. Later calculations by Radtke *et al.* [10] showed that in the linear transport regime the thermoelectric power factor in multilayer thermionic devices is smaller than that of the thermoelectric one, and thus the main advantage of superlattices is in the reduction of phonon thermal conductivity. Mahan and Vining in a subsequent publication reached the same conclusion [11]. This analysis was also based on linear transport and symmetric barriers. Linearized ballistic transport over the barrier was emphasized.

In contrast to the previous publications Shakouri *et al.* in 1999 proposed that tall barrier, highly degenerate superlattice structures can achieve thermoelectric power factors an order of magnitude higher than the bulk values [12]. In this paper electron transport perpendicular to superlattice direction is revisited. It is shown that highly degenerate semiconductors and metal-based superlattices in the quasilinear transport regime can achieve a thermoelectric power factor exceeding bulk values. The key requirement in the latter case is nonconservation of lateral momentum during the thermionic emission process. This will allow a much larger number of hot electrons to participate in the conduction process. In a separate publication, this theory for electron transport is compared with experimental I - V characteristics of $\text{InP}/\text{InGaAsP}$ HIT energy converters and the dark current for a variety of quantum well infrared photodetectors. A good fitting is found in a wide range of temperatures [13].

We first calculate the current-voltage characteristic and the energy transfer for a heterostructure superlattice device in the case of planar barriers and without significant scattering at interfaces.

In this case the longitudinal (z) component of the wave function can be separated from the other degrees of freedom, and the lateral momentum during thermionic emission is conserved [14]. We consider the case of thick barriers where tunneling current can be neglected. One can limit the analysis to two-dimensional density of states when the Fermi level is deep inside the well, similar to the case of quantum well intersubband photodetectors. However, the Fermi level in HIT energy converters is close to the top of the barrier and one needs to consider the contribution of the electronic states above the barrier.

Figure 1(a) shows a schematic energy diagram for two neighboring wells. E_1, E_2 , etc. are the quantized energy levels, E_f is the Fermi level, and E_b is the barrier height. Figure 1(b) shows k_1, k_2, k_f , and k_b , which are the wave vectors corresponding to the energies: $E_i = \hbar^2 k_i^2 / 2m$. From the energy diagram we can see that the barrier height is chosen so that only hot electrons with energies higher than the Fermi level are emitted over the barrier. The picture in the momentum space shows that many of the “hot” electrons that reside in volume V_2 but not in volume V_1 cannot be selectively emitted, since their component of momentum perpendicular to the plan (k_z) is not high enough to overcome the barrier. The number of electrons that participate in the thermionic emission process can be written directly as an integral in k_x, k_y, k_z space:

$$n_e(V) = \frac{2}{4\pi^2} \sum_{k_z} \int_{-\infty}^{\infty} dk_x \int_{-\infty}^{\infty} dk_y [f(k_x, k_y, k_z, E_f) - f(k_x, k_y, k_z, E_f - qV)] T(k_z, V) + \frac{2}{8\pi^3} \int_{k_b}^{\infty} dk_z \frac{\hbar^2 k_z^2}{m} \int_0^{\infty} dk_x \int_0^{\infty} dk_y \left(-\frac{\partial f}{\partial E} \right) T(k_x, k_y, k_z, V), \quad (1)$$

where f is the Fermi-Dirac distribution function, and V is the applied voltage across barrier. The first integral gives the contribution from the quantized energy levels of the well, corresponding to planes k_1 and k_2 in Fig. 1(b). Quantum mechanical transmission probability across the barrier, T , depends only on V and k_z value because we have assumed that the lateral momentum is conserved. The second integral is the number of transmitted electrons from the energy band above the barrier, corresponding to the states in volume V_1 in Fig. 1(b). For the latter electrons we assume a bulk-type Boltzmann transport with a correction due to quantum mechanical transmission above the barrier. To calculate the effective Seebeck coefficient, one needs to obtain the energy transported

by these electrons (n_Q). The equation for the calculation of n_Q is similar to Eq. (1) except that the integrand is multiplied by the difference of the energy of emitted electrons from the Fermi level: $\hbar^2(k_x^2 + k_y^2 + k_z^2 - k_F^2) / 2m$.

Interaction of the quantized charge carriers in the quantum well with inhomogeneities or a nonplanar barrier can couple the in-plane and perpendicular to the plane degrees of freedom. Thus, the conservation of lateral momentum could be broken during thermionic emission. In this case the transmission probability depends on the total energy of the electron and not just the kinetic energy perpendicular to the well [14–16]. One thus replaces $T(k_z, V)$ with $T(k_x, k_y, k_z, V)$ in the first term of Eq. (1), and all the states with $k > k_b$ will participate in transport. Thus, the integration volume is divided into two regions of $k_x^2 + k_y^2 + k_z^2 < k_b^2$ and $k_x^2 + k_y^2 + k_z^2 > k_b^2$ for the 2D and 3D states, respectively.

As a specific example, let us consider a 50 period 100 Å $\text{Hg}_{0.8}\text{Cd}_{0.2}\text{Te}/200$ Å $\text{Hg}_{0.2}\text{Cd}_{0.8}\text{Te}$ superlattice HIT energy converter. For this structure, barrier height, electron effective mass, mobility, and thermal conductivity are taken to be 642 meV, $0.015m_e$, $1 \text{ m}^2/\text{Vs}$, and 1 W/mK , respectively. Relatively thick barriers are used to have most of the contribution to current from thermionic emission above the barrier. Electronic states in the barrier region can be taken into account with the formalism of Ref. [13]. In Fig. 2 (top panel) we have plotted the effective conductivity of the considered HgCdTe superlattice at a bias of 0.15 V. One should note that Eq. (1) is nonlinear in the applied voltage and thus bias dependent conductivity can be defined. An effective Seebeck coefficient and thermoelectric figure of merit are also plotted in Fig. 2 for the three cases of bulk, superlattice when

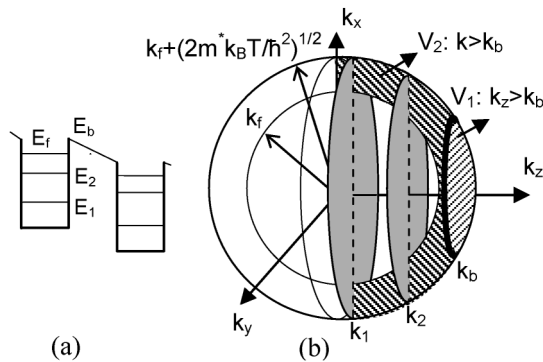


FIG. 1. (a) Conduction band and energy levels of two neighboring wells. (b) Corresponding wave vectors in the k space: k_1, k_2 , and k_b correspond to cross sectional planes and k_f is the radius of the Fermi sphere ($E_i = \hbar^2 k_i^2 / 2m$). V_1 is the volume of the electrons that participate in thermionic emission above the barrier if the lateral momentum is conserved ($k_z > k_b$). V_2 is that volume if the lateral momentum is not conserved ($k = \sqrt{k_x^2 + k_y^2 + k_z^2} > k_b$).

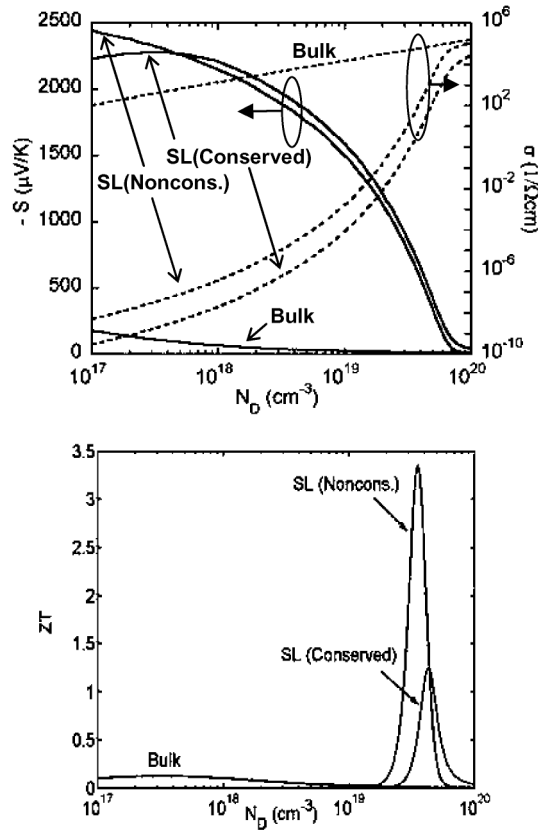


FIG. 2. Effective conductivity (dashed line) and Seebeck coefficient (solid line) (top panel), and ZT (bottom panel) versus doping for HgCdTe bulk, and superlattice assuming conserved and nonconserved lateral momentum.

lateral momentum is conserved, and superlattice when lateral momentum is not conserved.

We see that nonconservation of lateral momentum can significantly improve the performance of thermionic energy converters. It is important to note that thermal conductivity is often reduced in superlattice structures. To emphasize the cooling improvement solely due to the thermionic emission of electrons over the barrier, the reduced thermal conductivity is not included in the above analysis.

Now let us consider a more general point of view. In a thermoelectric energy converter, the working fluid is the electrons. They contribute to electrical conduction and they transport heat from one location to another. Since in conventional bulk or low-dimensional thermoelectrics, there is a trade-off between electrical conductivity and the Seebeck coefficient, there is an optimum doping on the order of $\sim 10^{18}$ – 10^{20} cm^{-3} . Because of this optimum doping, the focus of thermoelectric research has been on semiconductors since Ioffe's pioneering work in the 1950's. Since heat conduction in semiconductors is dominated by phonons, current research on thermoelectrics focuses on materials with low lattice thermal conductivity and high electrical conductivity [16,17]. On the other hand, metals have a large number of free electrons, which contribute to electrical conductivity, and they would be

ideal candidates for thermoelectric energy transport. However, metals have a very low Seebeck coefficient that results in a low thermoelectric figure of merit (ZT). The low Seebeck coefficient is due to the fact that when Fermi energy is deep inside the conduction band, the contribution of electrons with different energies to the conduction process (differential conductivity) is symmetric with respect to the Fermi energy (Fig. 3 top left). This could be explained by the fact that the number of available states in a typical 3D material scales with \sqrt{E} inside the conduction band. At high dopings, Fermi energy is deep in the band and density of states within the thermal energy range becomes more symmetric with respect to Fermi energy. The introduction of tall barriers inside metal will allow filtering of the hot electron and thus the Seebeck coefficient can be significantly increased (Fig. 3 top right). Thermal conductivity in metals is dominated by electron thermal conductivity that is approximately $2.44 \times 10^{-8} \sigma T$ in units of W/K according to the Wiedemann-Franz law. However, electrical conductivity (σ) in a tall barrier metallic superlattice is low

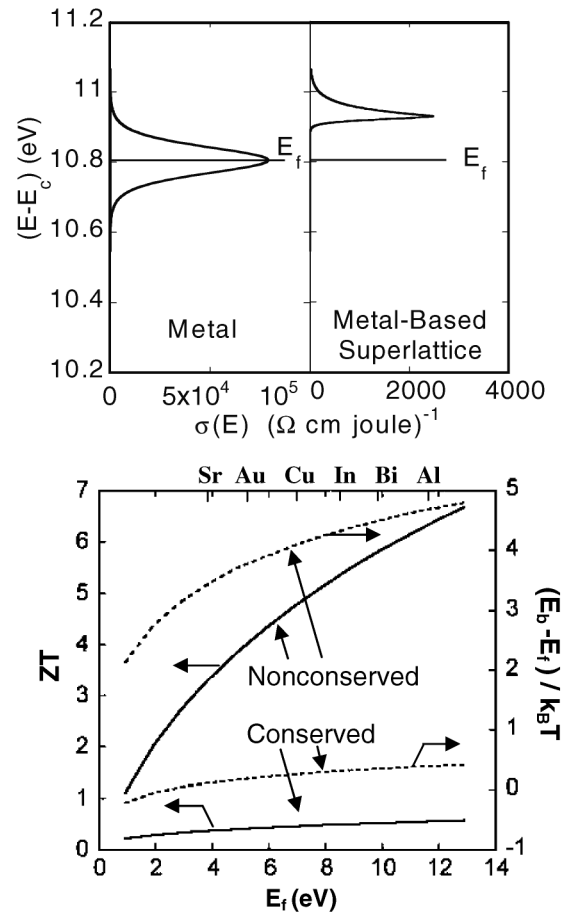


FIG. 3. Top panel: Differential conductivity versus electron energy in the conduction band for a bulk metal (left) and for a metal-based superlattice (right). Bottom panel: Thermoelectric figure of merit (left axis) and optimum barrier height (right axis) versus Fermi energy for a metal-based superlattice ($m^* = m_e$, $\mu = 12 \text{ cm}^2/\text{Vs}$, $\beta_{\text{lattice}} = 1 \text{ W/mK}$).

compared to that in bulk metal, and hence electron thermal conductivity can be comparable to that of phonons in the barrier. Therefore, ZT is also affected by the thermal conductivity of the barrier layer. Superlattice periods on the order of 5–20 nm are necessary in order to ensure adequate electron filtering above barriers. Thermal conductivity of such a composite material has not been investigated in detail. In a metal/insulator or metal/semiconductor superlattice, thermal conductivity of the metallic layer is dominated by the electron and that of the insulator/semiconductor layer by the lattice contribution. It will be interesting to study how heat is transported in such a structure and to look at interplay between electron and phonon contributions. Figure 3 bottom shows calculated thermoelectric figure of merit for a metal-based superlattice versus Fermi energy. Mobility is taken to be $12 \text{ cm}^2/\text{Vs}$ for a typical high electron density metal. The optimum barrier height with respect to Fermi energy in units of $k_B T$, which is needed to achieve maximum ZT , is shown on the right axis. One should notice that conservation of lateral momentum plays an important role to determine the number of carriers that participate in the conduction process. While ZT for the case of conserved lateral momentum remains less than 1 in this superlattice structure, it increases to about 7 for the case of non-conserved lateral momentum.

Moyzhes *et al.* used an argument based on energy relaxation length to show the potential of metallic superlattices for high figure-of-merit applications [18]. They mentioned the use of nonplanar interfaces to reduce metal/semiconductor electrical boundary resistance by increasing the effective surface area between the two layers. Unfortunately, the geometric argument for increased surface area neglects different length scales involved in electron transport and it does not include the correct number of electrons participating in conduction. Recent comprehensive transport calculations by Smith *et al.* showed that the experimental current-voltage characteristics in ballistic electron emission microscopy studies of Au/GaAs interfaces can be explained only when nonconservation of lateral momentum is taken into account [15]. Similar studies in epitaxial planar GaAs/AlGaAs heterostructures have shown that lateral momentum is mostly conserved [19]. Conservation of lateral momentum is a consequence of translational invariance in the plane of a quantum well. It is possible by introducing controlled roughness at interface to break this translational invariance and increase the thermionic cooling power density. It is important to note that the roughness can also decrease the electron mobility in the material and increase joule heating. However, experimental results with GaAs/InGaAs quantum dot infrared photodetectors show that it is possible to have lateral momentum nonconserved without affecting much the mobility of carriers moving above the barrier [20]. Controlled roughness of the superlattice interfaces during

the growth or taking advantage of quantum dot structures can create the required inhomogeneities [2].

In summary, we have given a detailed calculation of the thermionic current in HIT superlattice energy converters. In the case of nonconserved lateral momentum in the thermionic emission process, the number of hot electrons transmitted over the barrier can dramatically increase. With the use of highly degenerate semiconductors or metallic superlattices and tall barriers, $ZT > 5$ can be achieved with moderate lattice thermal conductivity of 1 W/mK .

The authors would like to acknowledge support from the Packard Foundation and the ONR Thermionic Energy Conversion Center MURI.

*Email address: ali@soe.ucsc.edu

- [1] R. Venkatasubramanian, E. Siivola, T. Colpitts, and B. O'Quinn, *Nature (London)* **413**, 597 (2001).
- [2] T. C. Harman, P. J. Taylor, M. P. Walsh, and B. E. LaForge, *Science* **297**, 2229 (2002).
- [3] G. D. Mahan, *J. Appl. Phys.* **76**, 4362 (1994).
- [4] A. Shakouri and J. E. Bowers, *Appl. Phys. Lett.* **71**, 1234 (1997).
- [5] A. Shakouri and J. E. Bowers, U.S. Patents No. 5955772 (1999) and No. 6060331 (2000).
- [6] M. D. Ulrich, P. A. Barnes, and C. B. Vining, *J. Appl. Phys.* **90**, 1625 (2001).
- [7] A. Shakouri and C. Labounty, in *Proceedings of the 18th International Conference on Thermoelectrics, Baltimore, 1999* (IEEE, Piscataway, NJ, 2000), pp. 35–39.
- [8] G. D. Mahan and L. M. Woods, *Phys. Rev. Lett.* **80**, 4016 (1998).
- [9] J. G. Kim *et al.*, in *Proceedings of the Material Research Society Spring Meeting, 2002* (Material Research Society, San Francisco, 2002), Abstract No. Z9.2, p. 391.
- [10] R. J. Radtke, H. Ehrenreich, and C. H. Grein, *J. Appl. Phys.* **86**, 3195 (1999).
- [11] G. D. Mahan and C. B. Vining, *J. Appl. Phys.* **86**, 6852 (1999).
- [12] A. Shakouri, C. Labounty, P. Abraham, J. Piprek, and J. E. Bowers, in *Materials Research Society Proceedings Vol. 545* (Materials Research Society, Pittsburgh, 1999), p. 449–458.
- [13] D. Vashaee and A. Shakouri, *J. Appl. Phys.* **95**, 1233 (2004).
- [14] S. V. Meshkov, *Sov. Phys. JETP* **64**, 1337 (1986).
- [15] D. L. Smith, E. Y. Lee, and V. Narayanamurti, *Phys. Rev. Lett.* **80**, 2433 (1998).
- [16] G. Chen and T. Zeng, *Microscale Thermophysical Engineering* **5**, 71 (2001).
- [17] G. Chen, *Semicond. Semimetals* **71**, 203 (2001).
- [18] B. Moyzhes and V. Nemchinsky, *Appl. Phys. Lett.* **73**, 1895 (1998).
- [19] V. Narayanamurti (private communication).
- [20] Shih-Yen Lin, Yao-Jen Tsai, and Si-Chen Lee, *Jpn. J. Appl. Phys.* **40**, L1290 (2001).